Combinatorial approach to the edge delamination test for thin film reliability—concept and simulation

Martin Y.M. Chiang*, Wen-li Wu, Jianmei He, Eric J. Amis

Polymers Division, National Institute of Standards and Technology, Gaithersburg, MD 20899, USA

Abstract

A high-throughput combinatorial approach to edge delamination test is proposed to map the failure of adhesion as a function of both temperature and film thickness in a single step. In this approach, a single specimen of a thin film bonded to a substrate with orthogonal thickness and temperature gradients is subdivided into separate samples. This approach can be adopted to measure the adhesion reliability for films with thicknesses in the nano regime by the addition of an overlayer. In addition, it can increase the pace of material innovations in nanoscale science and technology. The experimental requirements for a valid combinatorial test are analyzed using three-dimensional computational fracture mechanics. A simulation result is presented to demonstrate the feasibility of the combinatorial approach and to design the experimental protocol.
© 2003 Elsevier Science B.V. All rights reserved.

1. Introduction

The use of thin films (or coatings) in electronic packaging is growing rapidly with the introduction of new materials and processes combined with a better understanding of the background science. One area of concern for both customers and manufacturers in these applications is the reliability of the adhesion between film and substrate. For example, the next generation of electronic components will require new low dielectrics or other novel thin films to be integrated into their construction. In developing these new materials, it is important to assess the adhesion reliability in a fast, practical and reproducible fashion. The objective of this study is to develop a combinatorial or multivariant approach based on edge delamination to investigate the adhesion between a thin film and a substrate. This technique is expected to provide information about the interface integrity, adhesion and rate of material innovations (in this study, the adhesion means the debonding energy or the fracture toughness) [1–3]. More impor-

tantly, the proposed combinatorial approach can also be extended to measure the adhesion for films with thickness in the nanoscale regime, where the measurement of the adhesion for such thin films is very difficult.

The application of a combinatorial approach, which originally aimed at speeding synthesis and screening of large composition libraries for drugs and functional materials, has also enabled researchers to quickly evaluate how variables influence chemical and physical properties of materials and rapidly screen for optimal material properties [4–7]. In this study, a simulation combining fracture mechanics and three-dimensional finite element analyses was developed to evaluate the feasibility of the combinatorial approach outlined below.

During the cooling of a bi-material film/substrate system with an initial interfacial crack at a stress-free edge (Fig. 1), a further crack extension (debonding) along the interface will occur at a critical temperature due to the stress concentration near the crack tip. The edge delamination test is based on this debonding mechanism using the thermal stress generated during the cooling to cause separation of the film from the substrate. Accordingly, the adhesion (or adhesive strength) between the film coating and the substrate can

*Corresponding author. Tel.: +1-301-975-5186; fax: +1-301-975-4924.

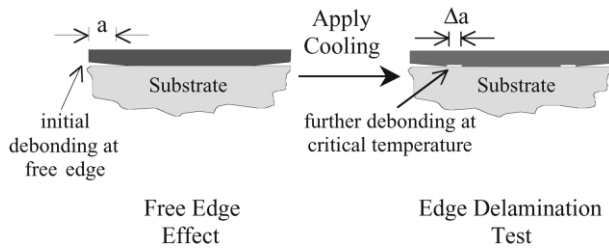*E-mail address:* martin.chiang@nist.gov (M.Y.M. Chiang).

Fig. 1. A two-dimensional schematic of the free edge effect and edge delamination test.

be deduced, e.g. Farris and Bauer [8]. By repeating the test for numerous samples with different film thicknesses, a distribution of failure (failure map, Fig. 2) as a function of temperature and film thickness can be constructed [9]. This failure map provides designing engineers a tool to assess the reliability limit of the coating. To construct a failure map to screen numerous new formulations and specialist materials is time-consuming. In this study, we propose to combine the important variables (temperature and thickness) in a single experiment to map the interfacial failure of the film. Subsequently, the value of adhesion of the film to substrate can be deduced from the failure map if the internal stress–temperature relation of the film is known. Essential details in the test design and requirements for valid testing results will be described in Section 2 of this article. Numerical results and discussion will be presented in Section 3.

2. Combinatorial approach to the edge delamination test

In the proposed experiment, a film is coated onto a relatively rigid substrate in such a way that the film has a thickness gradient in one direction (Fig. 3a). The film is cut into a square grid pattern to form an array of individual edge delamination samples on the substrate (Fig. 3b). The cut penetrates some distance into the substrate also. The edges are at 90° to the interface of the film/substrate. The depth (d) and width (w) of the cut are design parameters that need to be optimized and will be discussed later (Fig. 3c). Due to the existence of residual biaxial stresses during the solidification of the film and the stress-free edges after cutting in a bi-material system, stress concentrations arise at the interface near the free edges. These stress concentrations are sufficient to create small initial interfacial flaws at the film/substrate boundary. This is the well-known free-edge effect that is unique to bi-material systems [10–14]. Coupled with an interface having a finite adhesion strength, these initial flaws are the nucleation sites for interfacial debonding after a further loading. To introduce further loading, the specimen is cooled with a temperature gradient applied in the direction orthogonal
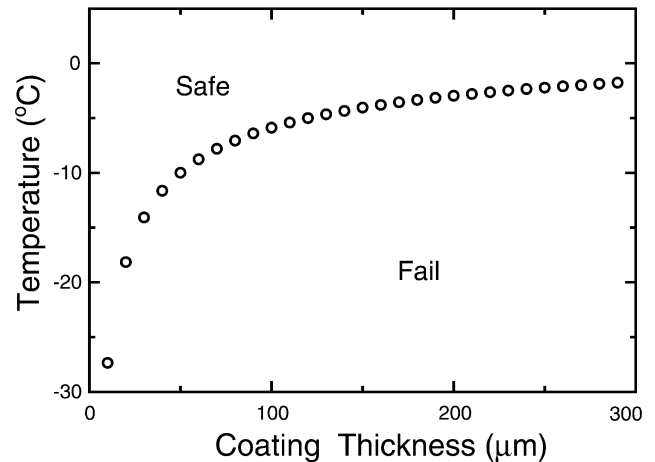

Fig. 2. A schematic of the failure map of a film on a substrate as a function of temperature and coat thickness.

to the thickness gradient (Fig. 3a). Interfacial debonding events will be observed for those samples having critical stresses that depend on the combination of local temperature and film thickness. Consequently, a failure map as a function of temperature and film thickness can be constructed with one step, as shown in Fig. 3a. In principle, if the adhesion of a film to a substrate is independent of temperature, the adhesion can be deduced from this failure map as long as the thermo-
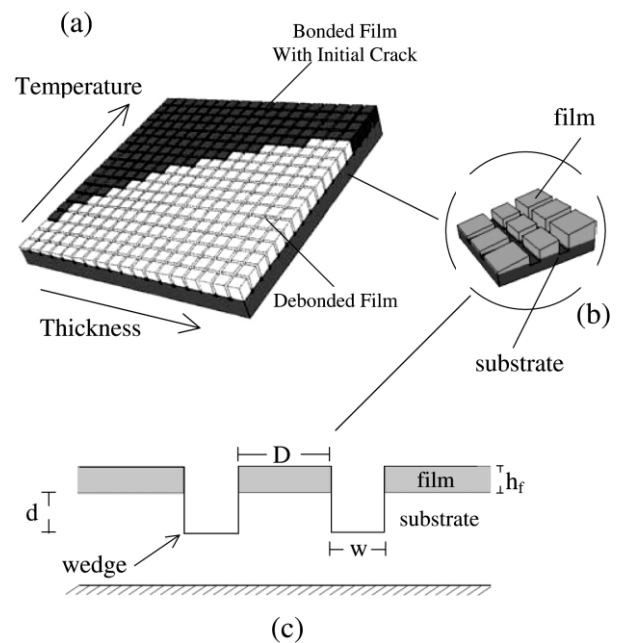

Fig. 3. A schematic of the combinatorial approach to the edge lift-off test: the multivariant specimen with film thickness and temperature gradients, and final failure map (a); a square pattern array of individual edge delamination samples on the substrate (b); the cutting depth, d, and width, w (c).
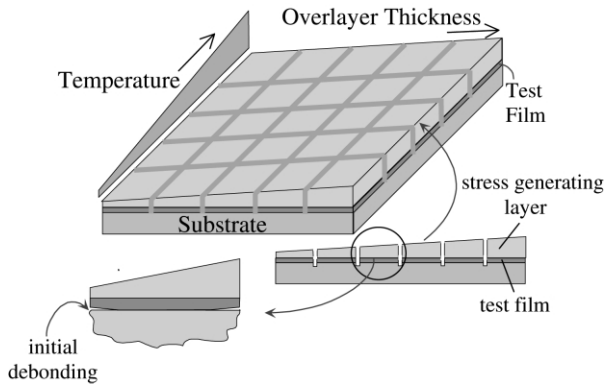
Fig. 4. A schematic of the combinatorial approach to the modified edge delamination test: the multivariant specimen with constant film thickness, overcoating layer thickness and temperature gradients.

mechanical property (the stress–temperature relation) of the test film is well characterized [9,15].

Sometimes, especially for large film thickness, the residual stresses (or internal energy) resulting from the solidification of the test film on a substrate (the film preparation step) could be large enough to cause premature failure of the film or interface before further cooling in the edge delamination test. Conversely, it could be the case that a film has such a strong bond with the substrate that the stress concentration generated during the cooling process is insufficient to induce debonding. In either case, by adjusting the film thickness and the upper and lower limits of temperature, one can ensure that the debonding condition will be met.

To measure the adhesion for films with thickness in sub-micron region, instead of coating a test film with a thickness gradient (Fig. 3a), a test film with a very small constant thickness is coated onto the substrate. Then, an overcoating layer (stress-generating layer) with a thickness gradient is deposited on the top of the thin test film (Fig. 4). The rest of the experimental procedures are identical with the original one. The thickness of the overcoating layer needs to be much larger than that of the test film such that the debonding energy contributed from the test film during the cooling can be neglected and only the overcoating layer serves as the stress-generating layer. One assumption in this modified approach is that the bonding strength between the test thin film and the overcoating layer is much higher than the bond between the test film and substrate. In this case, the stress–temperature relation of overcoating is only needed to calculate the adhesion. Consequently, one may use this modified combinatorial approach to obtain the critical bond energy for the thin film in the sub-micron range. It is worthwhile to note that once a well-characterized overcoating layer has been chosen, it can be used as a standard overcoating layer for different test films as long as good adhesion exists between the overcoating and the test films.

For the test results to be valid in this combinatorial edge delamination test, the stress state at the crack tip in each individual square sample must be independent of interfacial crack length. This requirement arises because the initial interfacial crack length in each sample cannot be well controlled. A second condition for validity of the test is that there must be no stress interaction among the separate edge delamination samples within one combinatorial specimen. Thus, two issues that must be determined to ensure valid test results are: the minimum initial crack length such that the stress states are independent of crack length (Fig. 1a), and the required cutting depth and width ('d' and 'w' in Fig. 3c) so that the stress interaction among separate edge delamination samples is negligible. A three-dimensional stress analysis (finite element method) and computational fracture mechanics were used to provide answers to these two important questions.

3. Results and discussion

The commercial finite element program, ABAQUS [16], was used to calculate the stress distribution in an edge delamination sample. A fully three-dimensional model of the combinatorial edge delamination specimen was constructed for the finite element analyses (FEA). For clarity, some of the FEA results and schematics are presented as two-dimensional schematics in this paper (e.g. Fig. 1). The film and substrate were assumed to be linearly elastic. The ratio of the film stiffness to the substrate stiffness was assumed to be 1:100 to reflect the relative rigidity of the substrate that will be discussed later in this article. This ratio also represents a typical organic overcoating on silicon substrate. The Poisson's ratios of the film and the substrate were assumed to be the same. The ratio of the coefficient of thermal expansion (CTE) of the film to the substrate was assumed to be 10 to mimic the mismatch of the CTEs. An initial crack was introduced along film/substrate interfaces to mimic the initial flaws; the length of this initial crack was varied to determine the region where the crack-tip stress is independent of crack length. The adhesion between the film and the substrate is assumed to be temperature independent.

The stress (or strain) distribution in linear elastic problems involving singularities can be well predicted from standard finite element techniques employing a non-singular finite element mesh, although convergence is very slow [13,17]. Therefore, no special elements were required in the analyses. Three-dimensional, 20-node isoparametric solid elements were used in this study, with the element dimensions continuously decreasing towards the crack tip. The mesh right at the crack tip was composed of square-grid elements having

a size of one twentieth of the film thickness. In order to make the comparisons on the stress distributions at the crack tip meaningful in parametric studies with different geometries (interfacial crack length, or cutting depth and width), a region enclosing the crack tip in the corner has been established with the same size for the finite element models. This region is a cube with the dimensions of four tenths of the film thickness. Within this region, the same number of elements (the same size of elements) has been assigned in the horizontal and the vertical directions for the models, and meshing varies only outside of this region. No crack tip blunting provisions were made in the finite element model.

Before performing systematic analyses, a study of solution convergence was carried out by employing various mesh refinements. The stress fields at the corner where two planar cracks meet were numerically evaluated as the average of the stress fields at the center of the elements immediately surrounding the crack tip. It was concluded from this study that good convergence of local strain was achieved. Based on the stress distribution along the interface, as a by-product of the convergence study, we determined that the size of each small square sample ('D' in Fig. 3c) should be larger than 20 times the film thickness in order to avoid the stress interaction between the corners in the sample. All the stress analyses performed in the study were based on the original combinatorial approach in which no overcoating layer is needed (only the test film with thickness gradient is present). The results of stress analyses should be applicable to the modified approach (a three-layer structure), since the test film thickness in the modified approach is much smaller than the overcoating layer.

Fig. 5 shows the variation of the stress normal to the interface at the corner of the sample as a function of the initial crack length. This normal stress is the driving force for interfacial debonding. The corner is where two interfacial cracks meet in the edge delamination sample, so the stress concentration is somewhat higher, and the cracks tend to propagate from the corner inward. The results in the figure indicate that the stress at the corner achieves nearly a steady state if the crack length is larger than 4% of the film thickness. An analysis of a two-dimensional crack (plane strain interface crack) shows that the steady state condition is only approached when the crack length is comparable to the film thickness [18]. The analysis performed in the present work suggests that the three-dimensional deformation field of the corner crack leads to steady state behavior at much shorter crack lengths than needed in the case of a two-dimensional crack. Thus, once the initial crack lengths of the individual edge delamination samples in the proposed combinatorial specimen are more than 4% of the film thickness, the stress states would be only a
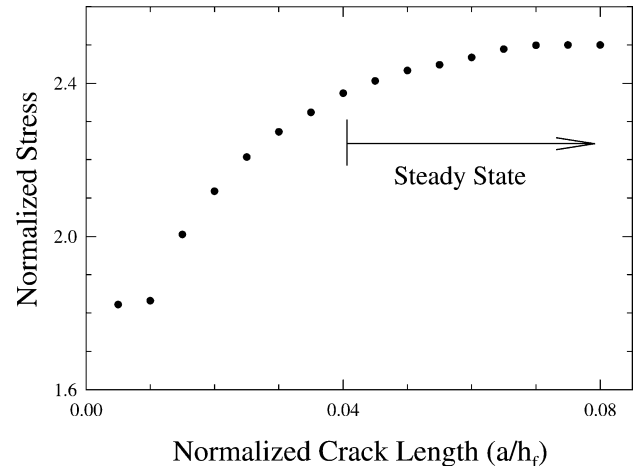

Fig. 5. The variation of the stress normal to the interface at the crack tip with the initial crack length. The stress is normalized by the applied stress.

function of temperature and film thickness. This requirement is not a significant barrier for using the proposed combinatorial approach since the initial debonding caused by the free-edge effect after cutting is typically longer than 4% of the film thickness. Chemical etching could also be used to obtain a suitable initial crack length if necessary.

Once the cutting penetrates into the substrate to form an array of individual edge delamination samples, it would create a wedge near 90° as shown in Fig. 3c. This wedge will induce a stress concentration during the cooling process due to the existence of a geometric discontinuity. The stress concentration could interfere with the stress state at the film/substrate interface. Also, the stress concentration at different wedges can interact with one another if the cutting width (Fig. 3c) is not large enough. This interaction could also translate into the interface and compound the stress states at the interface. Therefore, in order to make the stress state at the interface in each sample autonomous, the geometric parameters (w and d in Fig. 3c) have to be optimized. The contour plots shown in Fig. 6 qualitatively illustrate the stress interactions among the wedges resulting from cutting and the film/substrate interfaces for two adjacent samples. For comparison purposes, all the contour plots are displayed in the same scale. In the upper two plots in the figure, the ratio of the cutting depth to the film thickness (d/h_f) equals 0.1. On the left, where the ratio of the cutting width to the film thickness (w/h_f) equals 0.1, there is a stress interaction (overlap in darker colors in the contour plots) both between the interface and the wedge and between the wedge regions of adjacent samples. On the right, where w/h_f is 0.5, there is an interaction between the interface and the wedge, but no interaction between wedge regions of neighboring sam-
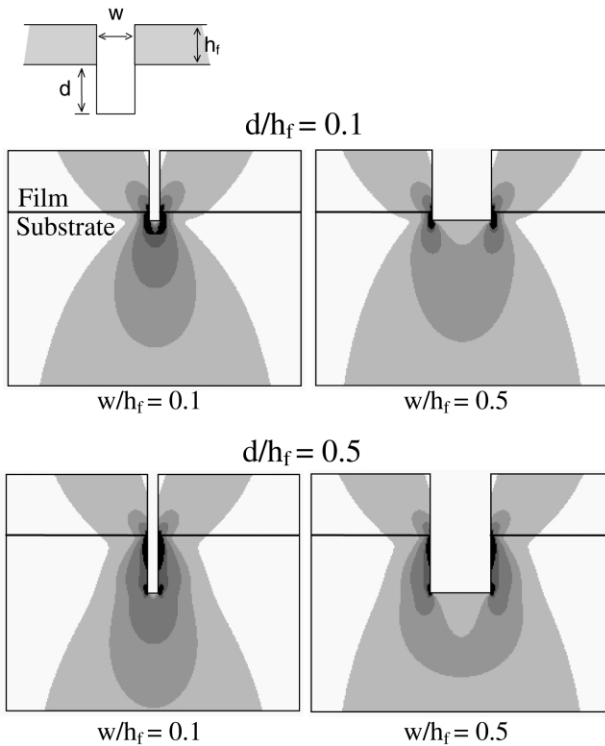
Fig. 6. The stress contours indicating the stress interaction among the cutting wedges and film/substrate interfaces for two adjacent specimens. The darker color indicates the stress concentration.

Fig. 7. The variation of the normal stress at the corner with the cutting width (w) as a function of the cutting depth (d).

ples. In the lower figures, where d/h_f is 0.5, it is observed from the contour plots that there is no interaction among any of the stress concentrations, even when w/h_f has been reduced to 0.1.

Fig. 7 shows the variation of the normal stress at the corner with cutting width (w) as a function of cutting depth (d). The results clearly demonstrate that when the cutting depth is greater than or equal to 50% of the film thickness, the normal stress at the corner is independent of cutting width. Experimentally, one would like to have the cutting width as small as possible in order to accumulate many samples on a single combinatorial specimen. Therefore, the results suggest that the cutting depth is a critical geometric parameter, which should be greater than half of the film thickness. In the figure, the deviation of the normal stress from a steady state (for $d/h_f=0.1$ or 0.3) implies that there is some influence on the stress state at the interface when the adjacent samples are close together. The difference in the magnitude of the steady state stress is evidence of the effect of the stress concentration from the cutting wedge on the interfacial stress state.

Based on these results for the geometric requirements, a simulation of the interfacial debonding of a combinatorial specimen having 6×6 individual edge delamination samples was carried out, as shown in Fig. 8. The film thickness varied from 20 μm to 200 μm. The

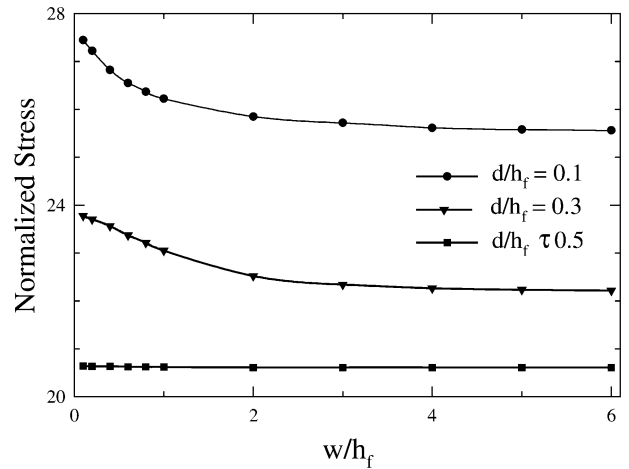temperature gradient was from −40 °C to −100 °C. The cutting depth was 100 μm and the cut width was 30 μm. For illustration purposes, the normal stress contours at the interface of the film/substrate are displayed in the figure (the specimen has been flipped over). The gradient of the film thickness is in the x_1 direction. The applied temperature gradient is in the x_2 direction. Each edge delamination sample provides four independent data points at the four corners, mapping the interfacial failure as a function of temperature and thickness. The darker color at the corner of each sample indicates that the stress state at the interface has exceeded the interfacial strength, which is a preset parameter in the simulation. By tracing the far field darker colors, a locus of failure (failure map) as a function of film thickness and temperature can be constructed.

During debonding of a film from a relatively rigid substrate, the contribution to energy release due to the substrate can be neglected. The energy release rate, G,
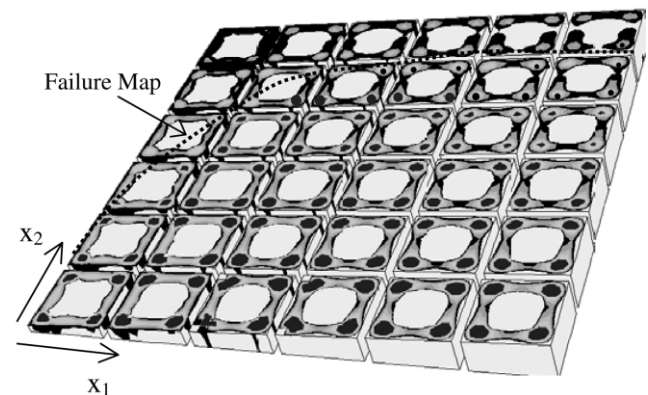

Fig. 8. The finite element simulation of interfacial debonding of a combinatorial specimen having 6×6 individual edge delamination samples.

associated with a plane–strain interface crack (2-D) between the film and the rigid substrate is [18]:

$$G = \frac{\sigma_0^2 h_f (1 - \nu_f^2)}{2E_f} \quad (1)$$

The subscript f represents the film. The parameters E, ν and h are the elastic modulus, Poisson's ratio and the thickness of the layers, respectively, and σ_0 is the internal stress. Also, with a relatively rigid substrate, the stress–temperature relation of a film on a substrate can be readily calculated through Stoney's equation, which is based on the curvature as a function of temperature for a coated bi-material circular plate (such as a film/substrate system) [15,19]. Consequently, using the failure map and the stress–temperature relation, through the analytical solution Eq. (1), the critical energy release rate can be calculated. A more rigorous on G 3-D solution can be obtained only through finite element analysis. Therefore, what is left is the definition of 'the relatively rigid substrate', which depends not only on the relative stiffness but also the relative thickness of a film/substrate system. This relative rigidity can be evaluated by the ratio of two parameters K and K^*, where

$$K = \frac{\overline{E_s}}{\overline{E_f}} \left(\frac{h_s}{h_f} \right) + 4 + 6\frac{h_f}{h_s} + 4\left(\frac{h_f}{h_s} \right)^2 + \frac{\overline{E_f}}{\overline{E_s}} \left(\frac{h_f}{h_s} \right)^3 \quad (2)$$

and

$$K^* = \frac{\overline{E_s}}{\overline{E_f}} \left(\frac{h_s}{h_f} \right) \quad (3)$$

where the subscript s represents the substrate. $\bar{E}$ [$=E/(1-\nu)$] is the bi-modulus of material. The parameter K is associated with the stress distribution of a bi-material plate due to a temperature change. For detailed explanation, readers may refer to Chiang et al. [15]. If $\bar{E}_s/\bar{E}_f$ $(h_s/h_f) \gg 1$ and $h_f/h_s < 1$, Eq. (2) is approximately the same as Eq. (3). This approximation is valid for many thin film applications where the film thickness is much smaller than that of the substrate. Also, the film stiffness is usually less than or comparable to that of the substrate. Therefore, the approximate equality between Eqs. (2) and (3) is a guideline for relative substrate rigidity. Fig. 9 presents the dependence of the ratio of K^*/K on the ratios of the film to substrate stiffness and of the film to substrate thickness. The relative rigidity can be assessed by the deviation of the K^*/K curve from $K^*/K = 1$. Accordingly, the appropriateness of using the failure map for deducing the adhesion can be evaluated. For example, when $h_f/h_s \leq 0.001$, the substrate can be considered as rigid even
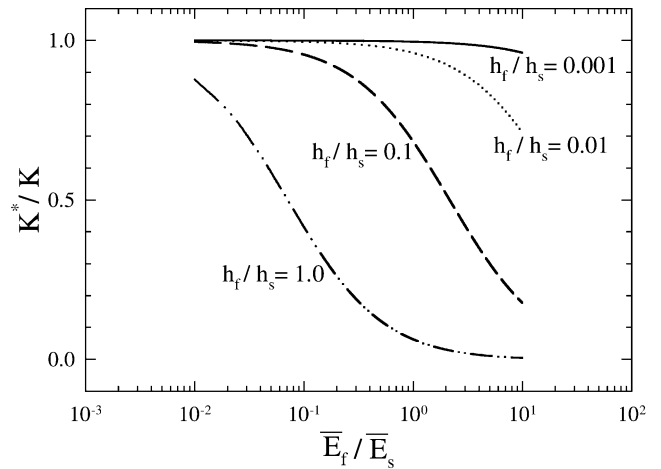

Fig. 9. The dependence of K^*/K on the ratios of the film to substrate stiffness and of the film to substrate thickness.

if the film rigidity is only one order of magnitude higher than that of the substrate.

4. Conclusions

A simulation, based on three-dimensional finite element modeling and fracture mechanics, has been carried out to demonstrate the feasibility and design of the experimental protocol for the combinatorial edge delamination test for thin film adhesion measurement. By combining variables that are important and readily controllable in practice (temperature and film thickness), the effect of stress concentration on the debonding of the film from the substrate is spatially varied in one experiment. Consequently, the failure map of the adhesion as a function of both film thickness and temperature can be constructed in a single step. This map of adhesion reliability can be used to determine the critical bond energy of the thin film in sub-micron thickness range. The approach is expected to provide accurate results because of its large sampling space. Necessary geometric parameters affecting debonding at the film/substrate interface are defined, and the validity of this combinatorial approach is successfully demonstrated in this study. Finally, this approach should be applicable to any film ranging from organic films (e.g. polymer) to inorganic films (e.g. metal or ceramic).

References

[1] K.L. Mittal, Pure Appl. Chem 52 (1980) 1295.
[2] K.L. Mittal, J. Adhes. Sci. Technol. 1 (1987) 247.
[3] L.P. Buchwalter, J. Adhes 72 (2000) 269.
[4] J.C. Zhao, Adv. Eng. Mater 3 (2001) 143.
[5] E.J. Amis, A. Sehgal, J.C. Meredith, A. Karim, Abstracts of Papers of the American Chemical Society 221:70-BTEC, Part 2, 2001.
[6] E.J. Amis, Abstracts of Papers of the American Chemical Society 222:339-Poly, Part 2, 2001.

[7] A.J. Crosby, A. Karim, E.J. Amis, Am. Chem. Soc. Polym. Prepr 42 (2001) 645.

[8] R.J. Farris, C.L. Bauer, J. Adhes 26 (1988) 293.

[9] E.O. Shaffer, F.J. McGarry, L. Hoang, Polym. Eng. Sci. 36 (1996) 2375.

[10] D.B. Bogy, J. Appl. Mech. 35 (1968) 460.

[11] R.B. Pipes, N.J. Pagano, J. Compos. Mater 4 (1970) 538.

[12] T.C.T. Ting, S.C. Chou, Int. J. Solids Struct 17 (1981) 1057.

[13] H.K. Stolarski, M.Y.M. Chiang, Int. J. Solids Struct 25 (1989) 75.

[14] T.C.T. Ting, Anisotropic Elasticity—Theory and Applications, Oxford University Press, Oxford, 1996.

[15] M.Y.M. Chiang, C.K. Chiang, W.L. Wu, J. Eng. Mater. Technol. Trans. ASME 124 (2002) 274.

[16] ABAQUS, Finite Element Analysis Code and Theory (Standard and CAE), Version 6.2, Hibbitt, Karlsson and Sorensen, Inc, RI, USA, 2000.
Certain commercial computer codes are identified in this paper in order to specify adequately the analysis procedure. In no case does such identification imply recommendation or endorsement by the National Institute of Standards and Technology (NIST) nor does it imply that they are necessarily the best available for the purpose.

[17] M.Y.M. Chiang, H. Chai, Int. J. Solids Struct 31 (1994) 2477.

[18] M.D. Thouless, H.C. Cao, P.A. Mataga, J. Mater. Sci 24 (1989) 1406.

[19] G.G. Stoney, Proc. R. Soc. Lond. Ser. A 82 (1909) 172.